

LatentSwap3D: Semantic Edits on 3D Image GANs

Enis Simsar¹ Alessio Tonioni² Evin Pınar Örnek¹ Federico Tombari^{1,2}

¹Technical University of Munich ²Google Switzerland

enis.simsar@tum.de alessiot@google.com evin.oernektum.de tombari@google.com

Abstract

Recent 3D-aware GANs rely on volumetric rendering techniques to disentangle the pose and appearance of objects, de facto generating entire 3D volumes rather than single-view 2D images from a latent code. Complex image editing tasks can be performed in standard 2D-based GANs (e.g., StyleGAN models) as manipulation of latent dimensions. However, to the best of our knowledge, similar properties have only been partially explored for 3D-aware GAN models. This work aims to fill this gap by showing the limitations of existing methods and proposing LatentSwap3D, a model-agnostic approach designed to enable attribute editing in the latent space of pre-trained 3D-aware GANs. We first identify the most relevant dimensions in the latent space of the model controlling the targeted attribute by relying on the feature importance ranking of a random forest classifier. Then, to apply the transformation, we swap the top-K most relevant latent dimensions of the image being edited with an image exhibiting the desired attribute. Despite its simplicity, LatentSwap3D provides remarkable semantic edits in a disentangled manner and outperforms alternative approaches both qualitatively and quantitatively. We demonstrate our semantic edit approach on various 3D-aware generative models such as π -GAN, GIRAFFE, StyleSDF, MVCGAN, EG3D, and VolumeGAN, and on diverse datasets, such as FFHQ, AFHQ, Cats, MetFaces, and CompCars. The project page can be found: <https://enisimsar.github.io/latentswap3d/>.

1. Introduction

In recent years there has been tremendous progress in Generative Adversarial Networks (GANs) focusing on synthesizing high-resolution and photorealistic images [17, 26–28]. It has been shown that manipulation of latent space results in semantically meaningful changes such as on rotation, brightness, shift x , shift y and zoom [24]. Furthermore, state-of-the-art semantic editing methods show that these latent spaces have robust control over the style of the generated images [39, 53, 54, 66]. These models reuse



Figure 1. Given an image we invert it in the latent space of a pre-trained MVCGAN [69] on FFHQ [27] enabling novel view synthesis. Then we use our LatentSwap3D to perform attribute editing (e.g., smiling). Row two and three show a comparison on this task between LatentSwap3D and StyleFlow [2].

pre-trained weights of generators for synthesizing high-resolution images and provide excellent attribute edits on 2D GANs [39, 53, 54, 66]. However, 2D GANs are developed without 3D-relevant characteristics, i.e., direct control over the camera pose and 3D shape of the generated object, and, therefore, struggle to generate consistent views of the same object from novel viewpoints.

Recently 3D-aware image synthesis GANs have been proposed to explicitly model objects' 3D shapes and pose as part of the image rendering process. Although powerful image editing methods exist for 2D generators, we have observed that their direct application falls short when applied to 3D GANs, as analysed in details in Sec. 4.2. We argue that this is due to the periodic latent spaces that many 3D-aware GAN methods build through sinusoidal activation functions [8, 18, 38, 69], which violate some of the algebraic assumptions behind existing edit methods for 2D GANs. A detailed analysis of the limitations of 2D image editing methods on 3D GANs is provided in the experiments.

Motivated by this, the goal of this work is to explore the capabilities of 3D-aware generative models for semantically meaningful edits of attributes, *e.g.*, in the case of face generation, *changing hair color, wearing eyeglasses, and smiling*. . . . We propose to achieve semantically meaningful edits on 3D generative models with sinusoidal latent spaces first by identifying possible dimensions in the latent code of 3D GANs which are strongly correlated with the desired attribute, then by appropriately tweaking them to achieve the desired visual effect. As shown in Fig. 1, our method outperforms the adaptation of StyleFlow [2] to MVCGAN [69] on the smiling editing task on real images.

Similar to their 2D counterpart, 3D-aware GANs expose different possible latent spaces that condition the image generation. Therefore, as a preliminary step to enable attribute edits, we identify the most suitable latent space by measuring their disentanglement, completeness, and informativeness (DCI), as proposed in [15] and firstly used in [61] in the context of measuring the quality of latent spaces of generative models. For the most suitable latent space, we want to identify which of its dimensions control the presence/absence of a specific attribute. To achieve that, we train a random forest [5] on top of latent codes to regress the presence/absence of the desired attribute. Once trained, the random forest provides a ranking of each feature based on its influence on the output label, therefore identifying which dimension(s) have more control on the specific edit. Given the latent code of an image we want to edit, we swap the top- K most relevant dimensions with the one of an image exhibiting the desired attribute, therefore applying the desired transformation. This explains why our method is dubbed LatentSwap3D. We show how the number K of swapped dimensions controls the intensity of the transformation. Furthermore, we propose a method to automatically tune K on a per-sample basis to apply the edit without altering the input image excessively. For example, one might want to tune K under the constraint of preserving the face identity for face editing purposes.

Our method is generalizable and can be applied to different 3D-aware generators and datasets without modification and without the need to fine-tune or re-train the generator part. We first show results for attribute editing of generated images from random seeds of the 3D-aware generators, then extend to attribute editing of real images. To do so, we invert the real image in the latent space of a 3D GAN, then apply LatentSwap3D to obtain a modified version exhibiting the desired attribute. Finally, we can render the image from arbitrary camera poses and extract the 3D model for downstream applications.

With the strategy explained in Sec. 3.1, LatentSwap3D allows obtaining a fully editable 3D model of a real object given only a single view. We test our method on top of state-of-the-art and commonly used models: π -

GAN [8], MVCGAN [69], EG3D [7], StyleSDF [38], GIRAFFE [37], StyleNeRF [18], VolumeGAN [63], and StyleGAN2 [27] generators trained on five public datasets: FFHQ [27], CelebA [32], AFHQ [10], CompCars [65], and MetFaces [25]. The main paper shows the editing results for π -GAN, MVCGAN, and EG3D on FFHQ, CelebA, Cats, and AFHQ datasets, while the remaining ones are included in the supplementary material. Our contributions can be summarized as follows:

- We explore the latent directions of 3D-aware GANs to determine their ability to encode semantically meaningful features.
- We propose LatentSwap3D enabling semantically meaningful attribute editing tasks for 3D-aware generative models without re-training the generators. Our method works for both sinusoidal latent spaces, such as π -GAN [8] and MVCGAN [69], and non-sinusoidal latent spaces such as EG3D [7].
- We extend LatentSwap3D to manipulate the attributes of real images using GAN inversion methods and successfully edit the attributes of real faces by simply varying their latent code.

2. Related Work

Image editing in GANs. StyleGAN generators [26–28] are arguably the most widely used methods for generating high-quality images. They have a mapping network that converts a random noise vector into a latent code that can encode semantically meaningful attributes [61]. Image manipulation can be implemented as manipulations of latent codes either supervised [2, 16, 53] or unsupervised [39, 54, 66]. Supervised methods are based on pre-trained attribute classifiers to predict the presence of semantic attributes. InterFaceGAN [53] uses pre-trained attribute classifiers, including age, hair color, and gender, to learn a hyperplane in latent space, whereas StyleFlow [2] employs normalizing flows that are attribute-conditioned and applies manipulation through condition labels. Unsupervised approaches, instead, do not require pre-trained classifiers. GANSpace [20] applies PCA over latent codes to obtain semantically meaningful edits, such as zoom, rotation, hair color, and gender. Semantic Factorization (SeFa) [54] finds semantic directions by retrieving eigenvectors from a projection matrix by singular value decomposition, whereas LatentCLR [66] uses a contrastive learning-based method. StyleCLIP [39] relies on the multimodal CLIP [45] to generalize to out-of-distribution semantic edits.

These editing methods have been mostly developed on top of StyleGAN and, as such, do not consider latent spaces defined by sinusoidal activation functions, which are periodic by design. Many 3D-aware models, however, use such

activations, and therefore the direct application of 2D edit methods causes unwanted effects, *e.g.*, significant identity change, degenerated facial attributes, and entangled edits.

3D-aware generative models. Current state-of-the-art GANs provide high-quality 2D images but cannot generate the underlying 3D structure of an object. Recently, however, the combination of NeRF with GANs has offered great potential for building 3D-aware generators [8, 18, 37, 50] that offer explicit control over the pose of the object in the image being generated. There are two trends for the architectures of 3D GANs: (i) **one-staged architecture**: use pure volumetric rendering in the generator and (ii) **two-staged architecture**: use a combination of low-resolution volumetric rendering and 2D GANs to increase the output resolution. GRAF [50] and π -GAN [8] are one-staged generators providing 3D-aware image and geometry generation using an implicit neural rendering but cannot afford high resolutions while training. Many two-staged generators [7, 18, 37, 38, 69] have been proposed to overcome this limitation. Among them StyleNeRF [18] and MVC-GAN [69] use NeRF-based 3D renderers, StyleSDF [38] uses Signed Distance Fields (SDF)-based 3D renderers as the first stage. Finally, EG3D [7] proposes hybrid explicit and implicit 3D representation through tri-plane. Notably, our method can work seamlessly with *all* of them, as demonstrated in the experimental results.

3D appearance & shape edits. Existing research on semantically meaningful edits methods for 3D shapes and appearances is limited, and many 2D image editing methods are not directly transferable to 3D-aware generators, as we experimentally show. StyleRig [59] uses StyleGAN [27] as a function to generate realistic faces from latent codes and optimizes a rig network to find semantic edits such as pose, expression, and illumination. MostGAN [34] has better pose, expression, and lighting results than StyleRig [59] but must be trained from scratch. ConfigNet [30] is a neural face image generator trained on both real and synthetic data [30]. Since its training process takes predefined labels, *e.g.*, facial hair and hair color, it can control the semantically meaningful edits during the generation process. However, it needs training from scratch, hence it is not possible to apply it to other pre-trained 3D-aware generative models. [31] showed high-quality and disentangled edits, such as *gender*, and *age*, using StyleFlow [2] on one of the state-of-the-art 3D-aware generator, EG3D [7]. However, we will show how StyleFlow underperforms with other 3D-aware generative models. FENeRF [58] and IDE-3D [57] propose 3D generators that enable portrait image editing by utilizing semantic maps. However, they need to train the generators from scratch and only apply them to existing generators after making significant changes in their architectures.

All the methods above are limited to manipulating the attributes of portrait images, *i.e.*, there is no application to other datasets like datasets that contain animal images [10, 68]. Moreover, some [30, 31] are limited to applying only specific types of GANs. In contrast, others [34, 59] have a limited amount of semantic edits, *e.g.*, pose, expression, and illumination.

Image inversion for generative models. Editing on real images is possible by obtaining the latent code for an input image by *GAN inversion*. There are different inversion approaches, from learning-based by using encoder networks [42, 47, 60] to optimization-based [1, 71] or hybrid [3, 70]. Several 3D-GAN inversion methods were recently proposed, including the optimization-based [8] and learning-based methods [6, 46].

3. LatentSwap3D

3.1. Overview

We aim to build a model agnostic method that can work on *any 3D-aware image generator*. Our method, LatentSwap3D, consists of two main components. The first one identifies important features in the latent space of a 3D GAN that controls the desired attribute through a random forest algorithm. Then, the target attribute is manipulated in an identity-preserving manner through a feature-swapping approach. An overview of the two components of LatentSwap3D can be seen in Fig. 2.

3.2. Background

Neural radiance fields (NeRFs) are represented as a set of multilayer perceptrons (MLPs), taking as input a 3D coordinate $\mathbf{x}, \mathbf{y}, \mathbf{z}$, and the camera azimuth and elevation angles (ϕ, θ) . The output is a spatially varying density and a viewpoint-dependent color. Finally, an image is rendered by sampling rays from the camera location towards the image plane and evaluating the corresponding radiance values [35].

3D-aware GANs like π -GAN build on top of the same volumetric rendering and aim to learn to generate NeRF-like volumes from a sampled a latent noise vector by training only on unlabelled 2D images. While for 2D gans, like StyleGAN [28], the generation process is controlled by Adaptive Instance normalization (AdaIN) [23], for 3D-GANs, such as π -GAN or MVCGAN, it is controlled through feature-wise linear modulation (FiLM) [43]. Formally, FiLM layers learn functions f and h which output $\gamma_{i,c}$ and $\beta_{i,c}$ as a function of input \mathbf{x}_i , $\gamma_{i,c} = f_c(\mathbf{x}_i)$ and $\beta_{i,c} = h_c(\mathbf{x}_i)$ where $\gamma_{i,c}$ and $\beta_{i,c}$ modulate a neural network’s activations $\mathbf{F}_{i,c}$ of i^{th} input’s c^{th} feature map, via a feature-wise affine transformation:

$$FiLM(\mathbf{F}_{i,c}|\gamma_{i,c},\beta_{i,c}) = \gamma_{i,c}\mathbf{F}_{i,c} + \beta_{i,c}. \quad (1)$$

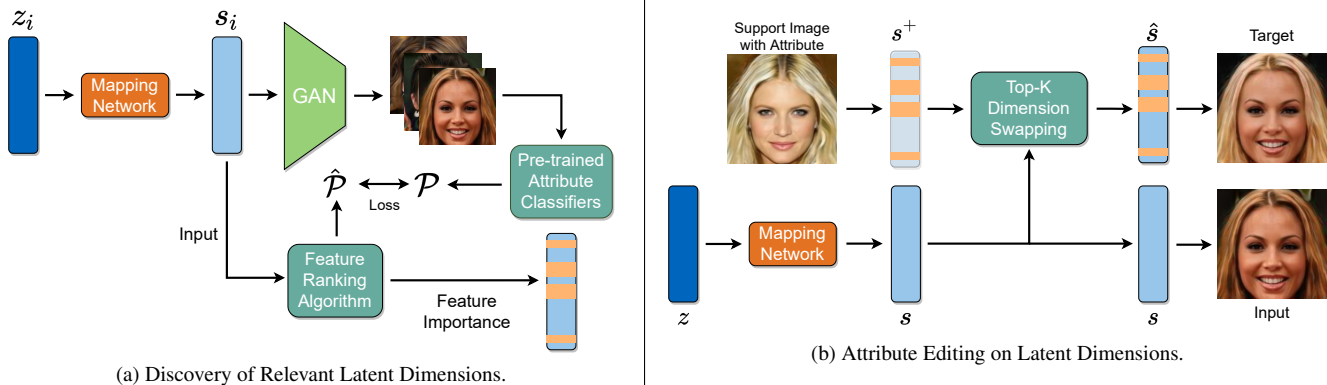


Figure 2. (a) We propose to train a random forest regressor taking latent codes s_i to predict the presence/absence of a desired attribute. We use the trained forest to rank the importance of dimensions of s_i with respect to the desired attribute. (b) Given the latent code s of an image, first, we find the closest latent code in the support set exhibiting the desired attribute (e.g., s^+ to increase *blondness*), then we swap the top K dimensions related to the attribute to generate an edited latent code \hat{s} that can be decoded in an edited image.

f and h can be arbitrary functions such as neural networks. In some 3D generators, like π -GAN, x_i is the position in space to render, and $\gamma_{i,c}$ and $\beta_{i,c}$ are obtained starting from an input latent code z and fed into a mapping network to guide the image generation process through SIREN [56] based FiLM layers:

$$\phi_i(x) = \sin(\text{FiLM}(\mathbf{F}_{i,c}|\gamma_{i,c}, \beta_{i,c})) \quad (2)$$

The underlying idea of having a mapping network reparametrizing the conditioning vector from a random multivariate normal distribution to a *modulation/style space* is shared across both 2D and 3D style-aware methods. However, the use of sine activation functions in 3D-aware models makes the latent space periodic and, therefore, more challenging to control with respect to one based on AdaIn layers. For instance, $\beta_{i,c}$ is the phase shift of a sine function and according to Eq. (2) will give the same output for every $\beta_{i,c} + 2k * \pi$ with $k \in \mathbb{Z}$. While, $\gamma_{i,c}$ controls the frequency of the sine function and affects the periodicity of the output. In practice, linear increases or decreases of $(\beta_{i,c}, \gamma_{i,c})$ might result in the opposite effect on the output of the sinusoidal activation. This makes some of the method proposals for the latent space of 2D GANs based on AdaIn layers fail. Since 3D-aware GANs include several latent spaces, the experimental section includes an analysis on their individual suitability for attribute editing.

3.3. Discovery of Relevant Latent Dimensions

The core idea of LatentSwap3D lies in using a feature ranking algorithm to determine the importance of features for a given attribute. In particular we rely on a random forest [5] for all the experiment in the main paper, but we will show results with other techniques in the supplementary material.

An overview of the process is summarized in Fig. 2a. To find relevant dimensions in the latent space of a 3D GAN,

we start by generating a set of images from randomly sampled latent codes. Then, we label the generated set using pre-trained image attribute classifiers to predict an attribute score for each image, i.e., \mathcal{P} in the figure. The scores correspond to the presence or absence of a particular attribute in the generated images. Since random forests are very effective models to rank feature importance, we train one to predict the presence/absence of an attribute from the generator latent codes. Finally, we use the occurrence with which a decision node of the forest selects the input dimensions to rank the relevance of each dimension concerning the presence/absence of a specific attribute [12].

3.4. Attribute Editing on Latent Dimensions

The existing 2D GAN manipulators perform semantic editing on latent spaces by applying algebraic operations. However, this is not applicable to 3D GAN models, as discussed in Sec. 3.2, since they rely on periodic non-linear spaces parametrized by a frequency and phase shift. Therefore, we propose to perform attribute editing by swapping relevant dimensions between the representation in the latent space of two samples.

We demonstrate the attribute editing process in Fig. 2b. After determining the ranking of latent dimensions for a given attribute with the random forest, LatentSwap3D replaces the top- K features of the latent code of an image being manipulated (s) with those of an image (s^+) taken from the support set used to train the random forest and exhibiting the desired attribute. The output latent codes (\hat{s}) generate the edited image with the desired attribute. In particular, we pick a support image whose attribute score is the lowest/highest for the desired attribute to add/remove the corresponding transformation to the manipulated image.

The parameter K should be carefully chosen for each transformation to preserve the identity of the generated im-

age after attribute editing. We use the identity loss \mathcal{L}_{ID} presented in Encoder4Editing [60] to automatically tune the parameter K on a per-sample basis. This loss calculates the cosine similarity between the feature embedding of the original image and that of the edited image. For example, in the face domain, we compute \mathcal{L}_{ID} based on a pre-trained ArcFace [13] face recognition network, while for other domains, a ResNet-50 network trained for MOCOv2 [9] is used. In particular, we select the maximum K that satisfies the constraint $\mathcal{L}_{ID} < \tau$.

We first select the top N images with the highest attribute score from the support set. Then, to maximize identity preservation, we choose the one most similar to the one currently being edited according to the distance between the respective latent codes as a support image for the swap. This process ensures that the dimensions will be swapped among similar samples sharing most attributes except the one we would like to modify.

3.5. 3D Edits on Real Images

Applying LatentSwap3D to a real image requires first GAN inversion [62] to embed it in the latent space of the pre-trained GAN generator. Moreover, inversion of 3D GANs additionally requires finding the camera pose from which the real image has been acquired [46].

For 3D GAN inversion, we follow an iterative optimization approach summarized in Fig. 3, where the latent vector and the pose are optimized alternatively. First, the latent vector is initialized to the mean vector in the latent space, while the camera pose is initialized to a neutral frontal position. Next, we start the inversion process by optimizing the camera location, c , while freezing the latent code, then we swap roles and tune the latent vector s , keeping the camera fixed. This process is repeated for the first 600 optimization steps. Then the camera is fixed while the latent code is further optimized for a fixed number of steps.

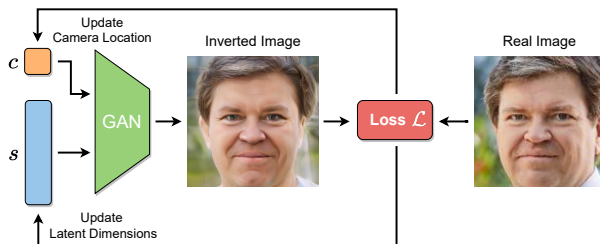


Figure 3. Inversion framework for a real image. s, c corresponds to the latent code and the camera location of the image, respectively. The loss is calculated between the inverted and real images.

We use a linear combination of reconstruction losses computed between the generated image and the reference one to guide the optimization: $\mathcal{L}_2, \mathcal{L}_{LPIPS}$ [67], and identity

Loss \mathcal{L}_{ID} [60]:

$$\mathcal{L} = \lambda_1 \mathcal{L}_2 + \lambda_2 \mathcal{L}_{LPIPS} + \lambda_3 \mathcal{L}_{ID} \quad (3)$$

where the values of λ s are specified in Sec. 4.

4. Experiments

We test our approach, LatentSwap3D, with three state-of-the-art 3D-aware generative models: π -GAN [8] used to develop the method, as a proof of concept, MVC-GAN [69] used to get high-fidelity images, and EG3D [7] used to show how our proposal can be applied also to networks with a non-sinusoidal-based latent space. The images used in the experiments are from four different datasets: Flickr-Faces-HQ (FFHQ) [27], Large-scale Celeb-Faces Attributes (CelebA) [32] Cats [68] and Animal Faces-HQ (AFHQ) [10].

π -GAN [8] is a NeRF-based one-staged 3D-aware generative model. A random noise vector $z \in \mathcal{Z}$ is first transformed into a 4608-dimensional vector $s \in \mathcal{S}$, corresponding to the frequency and phase shifts of FiLM layers. For π -GAN, we use this \mathcal{S} space to apply our edits.

MVCGAN [69] proposes a two-stage 3D-aware GAN. In the first stage, a neural volume renderer generates a low-resolution image and the geometry of a shape. In the second stage, a 2D styles-based generator enables high-resolution image generation. Its mapping network is converting from random noise $z \in \mathcal{Z}$ into intermediate latent codes $s \in \mathcal{S}$ conditioning the neural rendered. \mathcal{S} Space has 4864 dimensions and is the space we select to apply our edits.

EG3D [7] is also a two-stage 3D-aware GAN. Unlike MVCGAN, EG3D firstly feeds latent codes to a style-based 2D generator that predicts three orthogonal feature planes corresponding to the x, y, z axes of a 3D volume. Then, it uses a neural volumetric renderer to decode interpolated features from the three planes into a low-resolution image that later gets fed to a 2D super-resolution network. The mapping network of EG3D converts random noise $z \in \mathcal{Z}$, into intermediate latent codes $s \in \mathcal{S}$. \mathcal{S} space has 7168 dimensions and is the space we select to apply our edits.

Implementation. We investigate LatentSwap3D on 10K synthesized images for each dataset. For the face attributes, such as *gender, age, and hair color*, we use the pre-trained attribute models of the StyleGAN [28] linear separability metrics. For both Cats and AFHQ datasets, we train a model for each attribute using annotated data from PetFinder.my Adoption Prediction Dataset [44]. For the selection of the number of features K , we set τ to 0.25 for the face domain and 0.1 for other domains. The weights in Eq. (3) are tuned to $\lambda_1 = 1.0, \lambda_2 = 0.6$ and $\lambda_3 = 0.3$. To rank feature importance, we use the mean decrease in impurity and the Scikit-learn [41] implementation.

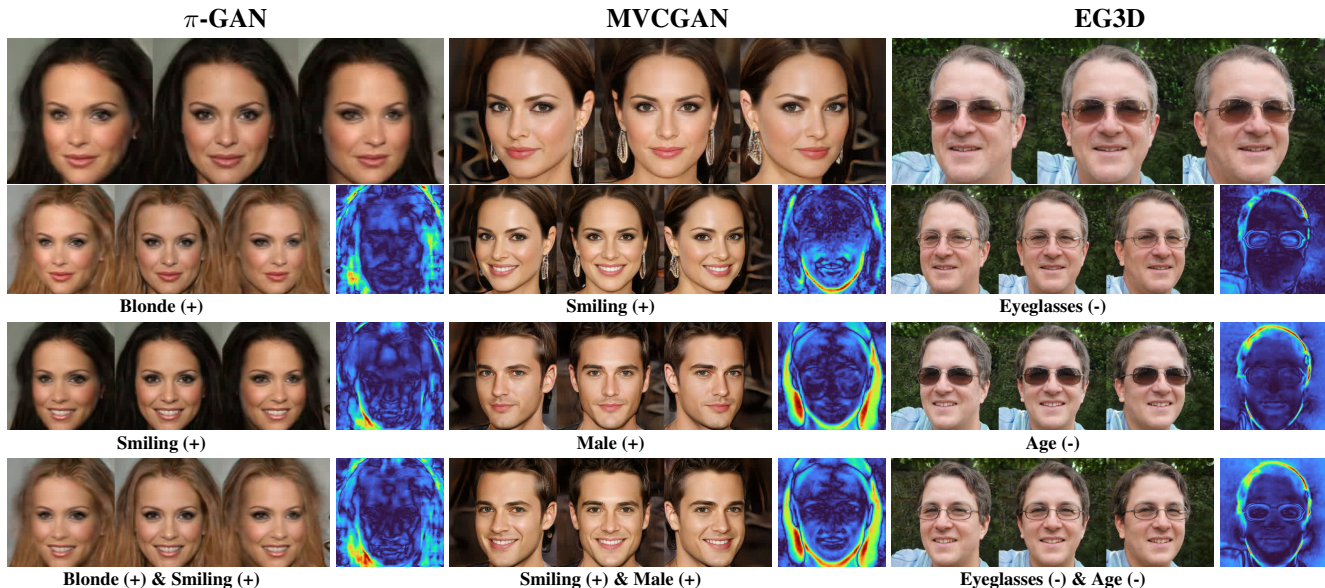


Figure 4. Qualitative results for our method, LatentSwap3D, on CelebA [32] with π -GAN [8], CelebA [32] with MVCGAN [69] and FFHQ [27] with EG3D [7]. A random seed image from different viewpoints is shown on the first row, followed by the edits for specific attributes and their combination in the last row, where (+/-) indicates an increase/decrease in the edited attribute. The rightmost column shows a heatmap of the changes in the underlying 3D geometry between the edited and original image.

4.1. Exploration of 3D GAN Latent Space

There is scarce research on exploring the latent spaces of 3D-aware generative models. Therefore, we started our work by evaluating the representative power of the different latent spaces by using the DCI metrics proposed in [15] and adapted in StyleSpace [61] to calculate the disentanglement, completeness, and informativeness of a latent space. We conduct preliminary experiments to identify each generator’s most suitable latent space. Results for the candidate latent spaces of π -GAN for CelebA, MVCGAN for CelebA, and EG3D for FFHQ are reported in Tab. 1.

Generator	Space	Disent. \uparrow	Compl. \uparrow	Inform. \uparrow
π -GAN	\mathcal{Z}	0.44	0.31	0.73
	\mathcal{S}	0.80	0.91	0.98
MVCGAN	\mathcal{Z}	0.43	0.30	0.75
	\mathcal{S}	0.85	0.91	0.97
EG3D	\mathcal{Z}	0.57	0.33	0.65
	\mathcal{W}	0.86	0.51	0.91

Table 1. Metrics for disentanglement, completeness and informativeness for the different latent spaces of π -GAN, MVCGAN and EG3D trained respectively on CelebA, CelebA and FFHQ. \mathcal{Z} space consists of the vectors sampled from a multivariate normal distribution. \mathcal{S} space denotes the frequency and phase shifts for π -GAN and MVCGAN. \mathcal{W} Space indicates the intermediate latent space of EG3D.

The training data of the DCI regressors are generated using 40 binary classifiers trained with the CelebA attributes [32] such as *blond hair*, *gender*, and *eyeglasses*. 10K random noise vectors, $z \in \mathcal{Z}$, are sampled from a multivariate normal distribution and fed into the corresponding generator to get latent codes and the generated images used to train the DCI regressors.

Table 1 shows how for π -GAN the \mathcal{S} space has significantly better values in terms of disentanglement, completeness, and informativeness. MVCGAN shares similar latent spaces to π -GAN, and the \mathcal{S} space is better than the \mathcal{Z} space. Finally, the DCI metrics for latent spaces of EG3D show that \mathcal{W} space is better than the initial latent space \mathcal{Z} . This indicates that intermediate spaces of these models better disentangle the attributes of the generated images.

4.2. Qualitative Evaluation

Edits of generated images. Figure 4 illustrates qualitative results on the CelebA dataset for π -GAN and MVCGAN, and FFHQ for EG3D, where we apply manipulations on attributes such as *blondness*, *smiling*, *changing gender*, *changing eyeglasses type*, and *age*. For these experiments we sample a seed image from a frontal viewpoint, extract the latent code, and apply semantic edit in the latent space. Finally, we render the edited face from multiple views. We observe that our method indeed enables attribute edits in a disentangled fashion while maintaining 3D consistency from multiple views.

We furthermore visualize 3D error maps to evaluate the

3D consistency, by extracting the depth maps from the underlying 3D geometry between the edited face and the original one and calculating the absolute depth differences. The rightmost column of Fig. 4 shows error maps in form of heat maps, and the color red indicates distinct changes. Especially in the case of MVCGAN, visual edits correspond nicely to actual changes in the underlying 3D geometry of the neural field (e.g., the smiling edit modifies the chin and lips of the person in 3D). We further observe that the semantic edit quality is naturally bounded by the 3D generator’s quality (e.g., heatmaps from π -GAN blonde and smiling are noisier).

In addition to face datasets (CelebA and FFHQ), we also demonstrate edits for Cats and AFHQ datasets in Fig. 5 to prove the applicability of our method to other datasets besides human faces. Fig. 5 show the results of π -GAN, MVCGAN, and EG3D on the Cats and AFHQ datasets. Our method can successfully modify the fur color and breed of the cat images.

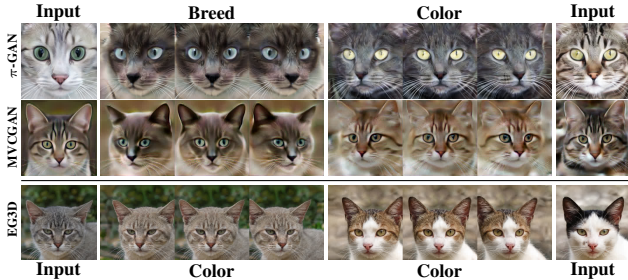


Figure 5. Results for Cats dataset [68] with π -GAN and AFHQ dataset [10] with MVCGAN and EG3D generators. Our proposed method, LatentSwap3D, is able to edit the breed and color of a generated image of a cat.

Editing of real images. As explained in Sec. 3.5, our method can work on real images captured from any viewpoint. Fig. 6 shows the semantic edits on samples inverted in the latent space of MVCGAN. Our proposed method successfully performs editing tasks for real faces.

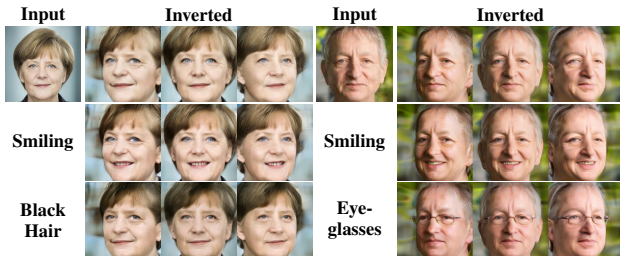


Figure 6. Inversion, editing and novel view synthesis for real images using our method and MVCGAN as generator.

2D editing methods on 3D-aware generative models. We compare our method with the state of the art 2D-based

latent space manipulators, namely, InterFaceGAN [53], SeFa [66], LatentCLR [54], and StyleFlow [2]. In Fig. 7, we show a smile edit on π -GAN, MVCGAN, and EG3D. For SeFa and LatentCLR we had to manually select identified directions that roughly correspond to the desired edits.

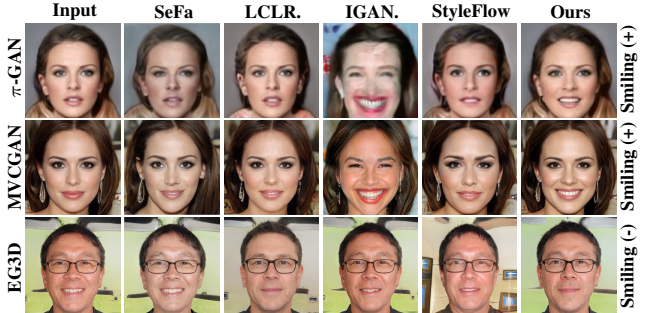


Figure 7. Comparison between InterFaceGAN [53], SeFa [54], LatentCLR [66], StyleFlow [2] and LatentSwap3D on π -GAN, MVCGAN, and EG3D models while performing a "smiling" edit.

Our method provides impressive results for π -GAN, MVCGAN, and EG3D generators, whereas the other methods sometimes result in nonsensical images or entangled edits. Since InterFaceGAN applies linear operations, if the coefficients of the manipulation are too large they might conflict with the periodicity of latent space and generate unnatural images (such as the face edit on π -GAN). StyleFlow changes the identity and fails to apply the desired attributes. On the other hand, SeFa and LatentCLR provide unsupervised edits, but there are no semantically meaningful edits, and sometimes they cannot preserve the identity.

Comparison of ConfigNet and LatentSwap3D. We compare our proposed method, LatentSwap3D, to ConfigNet [30], which is a neural face image generator developed to enable semantic edits. ConfigNet has been explicitly trained to manipulate certain attributes and it requires a high amount of synthetic data, while LatentSwap3D finds the latent codes that enable the semantically meaningful edits on images without re-training the generative models.

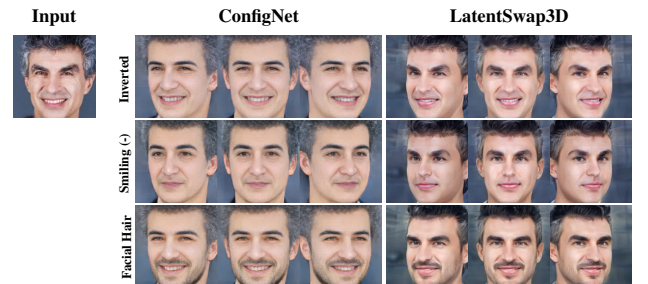


Figure 8. Comparison of ConfigNet [30] and our method on smiling and facial hair attributes for a real face image.

Figure 8 shows real images attribute editing of the two methods for smiling (+) and facial hair. We first observe that the inversion quality of real images in LatentSwap3D is better than the ConfigNet method. Moreover, as the realism of semantic edits is tightly coupled to inversion quality, our LatentSwap3D generates more realistic edited images which preserve the identity of the subject.

Proposed method on StyleGAN2. LatentSwap3D is not limited to 3D-aware GANs but also works on image-based GANs like StyleGAN2, see Fig. 9. First, by applying the same procedure in Sec. 3.3, we identify the latent codes from the style space of StyleGAN2 that are most important for the desired attribute. Then, we swap these latent codes to generate the desired edits, as explained in Sec. 3.4.

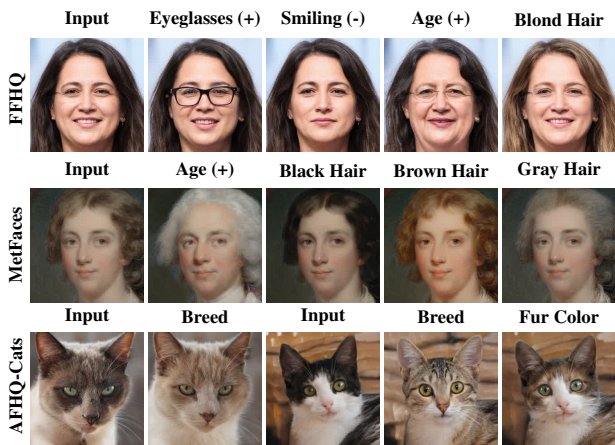


Figure 9. LatentSwap3D attribute editings on StyleGAN2 [28] for AFHQ dataset [10], MetFaces dataset [25], and FFHQ [27].

4.3. Quantitative Evaluation

Semantic Correctness. To evaluate the effectiveness of our attribute edits quantitatively, we use a pre-trained smile attribute classifier [52] to measure the percentage of smiling images in a set of 2500 images of not smiling faces. We edit the images with different methods and measure the increase in percentage. With π -GAN, our method increases the percentage of smiling images by 84% whereas InterFaceGAN and StyleFlow increase only by 76%, and 78%, respectively. The same improvement applies to images generated by MVCGAN and EG3D. Percentages of improvement for each of them are 92%, and 84%, respectively. For the details, see Tab. 2.

Identity preservation. We measure the identity stability between original and edited images using an identity verification tool [52] based on FaceNet512 [49]. Table 3 shows the identity preservation metric on 10K images, and compared to the other methods, after applying edits, our method is the best to preserves the identity of the original image.

	π -GAN	MVCGAN	EG3D
Unedited Images	4%	3%	9%
InterFaceGAN [53]	81%	84%	66%
StyleFlow [2]	83%	78%	74%
Ours (LatentSwap3D)	88%	95%	93%

Table 2. Quantitative comparison of semantic correctness metric among different image editing methods for π -GAN [8], MVCGAN [69], and EG3D [7] on smiling attribute edits of face images.

	π -GAN	MVCGAN	EG3D
LatentCLR [54]	54%	61%	69%
SeFa [66]	62%	64%	58%
InterFaceGAN [53]	30%	51%	70%
StyleFlow [2]	68%	65%	71%
Ours (LatentSwap3D)	74%	71%	73%

Table 3. Quantitative comparison of identity preservation metric among different image editing methods for π -GAN [8], MVCGAN [69], and EG3D [7] on several attribute edits of face images.

5. Conclusions

To the best of our knowledge, we proposed the first generalized editing method to enable semantic manipulation for 3D GANs, which is both *generator* and *dataset* agnostic as shown through various models (*e.g.*, π -GAN, GIRAFFE, StyleSDF, MVCGAN, EG3D, and VolumeGAN) and datasets (*e.g.*, FFHQ, AFHQ, Cats, MetFaces, and CompCars). Furthermore, our method enables complex edits and multi-view consistent rendering from a single image of a real face or an object, opening the path to multiple practical applications. The broader impact of this work includes possible use cases in compression for video conferencing or 3D manipulation for AR overlays. On the other hand, like all GAN-based image editing methods, LatentSwap3D will suffer from datasets bias and is limited by the images that can be modeled by the GAN being manipulated. However, considering the rapid progress in generative modeling and the generality of our proposed framework, we envision that our method will be equally applicable in future generations of generative models, resulting in even more impressive editing capabilities.

Acknowledgments We are grateful to Google University Relationship GCP Credit Program for the support of this work by providing computational resources.

References

- [1] Rameen Abdal, Yipeng Qin, and Peter Wonka. Image2stylegan: How to embed images into the stylegan latent space? In *Proceedings of the IEEE/CVF International Conference on Computer Vision*, pages 4432–4441, 2019.
- [2] Rameen Abdal, Peihao Zhu, Niloy J Mitra, and Peter Wonka. Styleflow: Attribute-conditioned exploration of stylegan-generated images using conditional continuous normalizing flows. *ACM Transactions on Graphics (TOG)*, 40(3):1–21, 2021.
- [3] David Bau, Jun-Yan Zhu, Jonas Wulff, William Peebles, Hendrik Strobelt, Bolei Zhou, and Antonio Torralba. Seeing what a gan cannot generate. In *Proceedings of the IEEE/CVF International Conference on Computer Vision*, pages 4502–4511, 2019.
- [4] Mikolaj Bińkowski, Dougal J. Sutherland, Michael Arbel, and Arthur Gretton. Demystifying MMD GANs. In *International Conference on Learning Representations (ICLR)*, 2018.
- [5] Leo Breiman. Random forests. *Machine learning*, 45(1):5–32, 2001.
- [6] Shengqu Cai, Anton Obukhov, Dengxin Dai, and Luc Van Gool. Pix2nerf: Unsupervised conditional π -gan for single image to neural radiance fields translation. *arXiv preprint arXiv:2202.13162*, 2022.
- [7] Eric R Chan, Connor Z Lin, Matthew A Chan, Koki Nagano, Boxiao Pan, Shalini De Mello, Orazio Gallo, Leonidas Guibas, Jonathan Tremblay, Sameh Khamis, et al. Efficient geometry-aware 3d generative adversarial networks. *arXiv preprint arXiv:2112.07945*, 2021.
- [8] Eric R Chan, Marco Monteiro, Petr Kellnhofer, Jiajun Wu, and Gordon Wetzstein. pi-gan: Periodic implicit generative adversarial networks for 3d-aware image synthesis. In *Proceedings of the IEEE/CVF conference on computer vision and pattern recognition*, pages 5799–5809, 2021.
- [9] Xinlei Chen, Haoqi Fan, Ross Girshick, and Kaiming He. Improved baselines with momentum contrastive learning. *arXiv preprint arXiv:2003.04297*, 2020.
- [10] Yunjey Choi, Youngjung Uh, Jaejun Yoo, and Jung-Woo Ha. Stargan v2: Diverse image synthesis for multiple domains. In *Proceedings of the IEEE Conference on Computer Vision and Pattern Recognition*, 2020.
- [11] Corinna Cortes and Vladimir Vapnik. Support-vector networks. *Machine learning*, 20(3):273–297, 1995.
- [12] Antonio Criminisi and Jamie Shotton. *Decision forests for computer vision and medical image analysis*. Springer Science & Business Media, 2013.
- [13] Jiankang Deng, Jia Guo, Xue Niannan, and Stefanos Zafeiriou. Arcface: Additive angular margin loss for deep face recognition. In *CVPR*, 2019.
- [14] Yu Deng, Jiaolong Yang, Sicheng Xu, Dong Chen, Yunde Jia, and Xin Tong. Accurate 3d face reconstruction with weakly-supervised learning: From single image to image set. In *IEEE Computer Vision and Pattern Recognition Workshops*, 2019.
- [15] Cian Eastwood and Christopher KI Williams. A framework for the quantitative evaluation of disentangled representations. In *International Conference on Learning Representations*, 2018.
- [16] Lore Goetschalckx, Alex Andonian, Aude Oliva, and Phillip Isola. Ganalyze: Toward visual definitions of cognitive image properties. In *Proceedings of the IEEE/CVF International Conference on Computer Vision*, pages 5744–5753, 2019.
- [17] Ian Goodfellow, Jean Pouget-Abadie, Mehdi Mirza, Bing Xu, David Warde-Farley, Sherjil Ozair, Aaron Courville, and Yoshua Bengio. Generative adversarial nets. In Z. Ghahramani, M. Welling, C. Cortes, N. D. Lawrence, and K. Q. Weinberger, editors, *Advances in Neural Information Processing Systems 27*, pages 2672–2680. Curran Associates, Inc., 2014.
- [18] Jiatao Gu, Lingjie Liu, Peng Wang, and Christian Theobalt. Stylenerf: A style-based 3d-aware generator for high-resolution image synthesis. *arXiv preprint arXiv:2110.08985*, 2021.
- [19] Ligong Han, Sri Harsha Musunuri, Martin Renqiang Min, Ruijiang Gao, Yu Tian, and Dimitris Metaxas. Ae-stylegan: Improved training of style-based auto-encoders. In *Proceedings of the IEEE/CVF Winter Conference on Applications of Computer Vision*, pages 3134–3143, 2022.
- [20] Erik Härkönen, Aaron Hertzmann, Jaakko Lehtinen, and Sylvain Paris. Ganspace: Discovering interpretable gan controls. *arXiv preprint arXiv:2004.02546*, 2020.
- [21] Kaiming He, Xiangyu Zhang, Shaoqing Ren, and Jian Sun. Deep residual learning for image recognition. In *Proceedings of the IEEE conference on computer vision and pattern recognition*, pages 770–778, 2016.
- [22] Martin Heusel, Hubert Ramsauer, Thomas Unterthiner, Bernhard Nessler, and Sepp Hochreiter. Gans trained by a two time-scale update rule converge to a local nash equilibrium. *arXiv preprint arXiv:1706.08500*, 2017.
- [23] Xun Huang and Serge Belongie. Arbitrary style transfer in real-time with adaptive instance normalization. In *IEEE International Conference on Computer Vision (ICCV)*, pages 1501–1510, 2017.
- [24] Ali Jahanian, Lucy Chai, and Phillip Isola. On the “steerability” of generative adversarial networks. *arXiv preprint arXiv:1907.07171*, 2019.
- [25] Tero Karras, Miika Aittala, Janne Hellsten, Samuli Laine, Jaakko Lehtinen, and Timo Aila. Training generative adversarial networks with limited data. In *Advances in Neural Information Processing Systems (NeurIPS)*, 2020.
- [26] Tero Karras, Miika Aittala, Samuli Laine, Erik Härkönen, Janne Hellsten, Jaakko Lehtinen, and Timo Aila. Alias-free generative adversarial networks. In *Advances in Neural Information Processing Systems (NeurIPS)*, 2021.
- [27] Tero Karras, Samuli Laine, and Timo Aila. A style-based generator architecture for generative adversarial networks. In *IEEE Conference on Computer Vision and Pattern Recognition (CVPR)*, 2019.

- [28] Tero Karras, Samuli Laine, Miika Aittala, Janne Hellsten, Jaakko Lehtinen, and Timo Aila. Analyzing and improving the image quality of StyleGAN. In *IEEE Conference on Computer Vision and Pattern Recognition (CVPR)*, 2020.
- [29] Diederik P Kingma and Jimmy Ba. Adam: A method for stochastic optimization. *arXiv preprint arXiv:1412.6980*, 2014.
- [30] Marek Kowalski, Stephan J. Garbin, Virginia Estellers, Tadas Baltrušaitis, Matthew Johnson, and Jamie Shotton. Config: Controllable neural face image generation. In *European Conference on Computer Vision (ECCV)*, 2020.
- [31] Connor Z. Lin, David B. Lindell, Eric R. Chan, and Gordon Wetzstein. 3d gan inversion for controllable portrait image animation, 2022.
- [32] Ziwei Liu, Ping Luo, Xiaogang Wang, and Xiaoou Tang. Deep learning face attributes in the wild. In *IEEE International Conference on Computer Vision (ICCV)*, 2015.
- [33] Scott M. Lundberg, Gabriel Erion, Hugh Chen, Alex De-Grave, Jordan M. Prutkin, Bala Nair, Ronit Katz, Jonathan Himmelfarb, Nisha Bansal, and Su-In Lee. From local explanations to global understanding with explainable ai for trees. *Nature Machine Intelligence*, 2(1):2522–5839, 2020.
- [34] Safa C. Medin, Bernhard Egger, Anoop Cherian, Ye Wang, Joshua B. Tenenbaum, Xiaoming Liu, and Tim K. Marks. Most-gan: 3d morphable stylegan for disentangled face image manipulation, 2021.
- [35] Ben Mildenhall, Pratul P Srinivasan, Matthew Tancik, Jonathan T Barron, Ravi Ramamoorthi, and Ren Ng. NeRF: Representing scenes as neural radiance fields for view synthesis. In *European Conference on Computer Vision (ECCV)*, 2020.
- [36] Myauto.ge cars dataset.
- [37] Michael Niemeyer and Andreas Geiger. GIRAFFE: Representing scenes as compositional generative neural feature fields. In *IEEE Conference on Computer Vision and Pattern Recognition (CVPR)*, 2021.
- [38] Roy Or-El, Xuan Luo, Mengyi Shan, Eli Shechtman, Jeong Joon Park, and Ira Kemelmacher-Shlizerman. Stylesdf: High-resolution 3d-consistent image and geometry generation. *arXiv e-prints*, pages arXiv–2112, 2021.
- [39] Or Patashnik, Zongze Wu, Eli Shechtman, Daniel Cohen-Or, and Dani Lischinski. Styleclip: Text-driven manipulation of stylegan imagery. In *Proceedings of the IEEE/CVF International Conference on Computer Vision*, pages 2085–2094, 2021.
- [40] Karl Pearson. X. on the criterion that a given system of deviations from the probable in the case of a correlated system of variables is such that it can be reasonably supposed to have arisen from random sampling. *The London, Edinburgh, and Dublin Philosophical Magazine and Journal of Science*, 50(302):157–175, 1900.
- [41] F. Pedregosa, G. Varoquaux, A. Gramfort, V. Michel, B. Thirion, O. Grisel, M. Blondel, P. Prettenhofer, R. Weiss, V. Dubourg, J. Vanderplas, A. Passos, D. Cournapeau, M. Brucher, M. Perrot, and E. Duchesnay. Scikit-learn: Machine learning in Python. *Journal of Machine Learning Research*, 12:2825–2830, 2011.
- [42] Guim Perarnau, Joost Van De Weijer, Bogdan Raducanu, and Jose M Álvarez. Invertible conditional gans for image editing. *arXiv preprint arXiv:1611.06355*, 2016.
- [43] Ethan Perez, Florian Strub, Harm de Vries, Vincent Dumoulin, and Aaron C. Courville. Film: Visual reasoning with a general conditioning layer. In *AAAI*, 2018.
- [44] Petfinder.my adoption prediction.
- [45] Alec Radford, Jong Wook Kim, Chris Hallacy, Aditya Ramesh, Gabriel Goh, Sandhini Agarwal, Girish Sastry, Amanda Askell, Pamela Mishkin, Jack Clark, Gretchen Krueger, and Ilya Sutskever. Learning transferable visual models from natural language supervision, 2021.
- [46] Pierluigi Zama Ramirez, Diego Martin Arroyo, Alessio Tonioni, and Federico Tombari. Unsupervised novel view synthesis from a single image, 2021.
- [47] Elad Richardson, Yuval Alaluf, Or Patashnik, Yotam Nitzan, Yaniv Azar, Stav Shapiro, and Daniel Cohen-Or. Encoding in style: a stylegan encoder for image-to-image translation. In *Proceedings of the IEEE/CVF Conference on Computer Vision and Pattern Recognition*, pages 2287–2296, 2021.
- [48] Daniel Roich, Ron Mokady, Amit H Bermano, and Daniel Cohen-Or. Pivotal tuning for latent-based editing of real images. *arXiv preprint arXiv:2106.05744*, 2021.
- [49] Florian Schroff, Dmitry Kalenichenko, and James Philbin. Facenet: A unified embedding for face recognition and clustering. In *Proceedings of the IEEE conference on computer vision and pattern recognition*, pages 815–823, 2015.
- [50] Katja Schwarz, Yiyi Liao, Michael Niemeyer, and Andreas Geiger. GRAF: Generative radiance fields for 3D-aware image synthesis. In *Advances in Neural Information Processing Systems (NeurIPS)*, 2020.
- [51] Maximilian Seitzer. pytorch-fid: FID Score for PyTorch. <https://github.com/mseitzer/pytorch-fid>, 8 2020. Version 0.1.1.
- [52] Sefik Ilkin Serengil and Alper Ozpinar. Hyperextended lightface: A facial attribute analysis framework. In *2021 International Conference on Engineering and Emerging Technologies (ICEET)*, pages 1–4. IEEE, 2021.
- [53] Yujun Shen, Ceyuan Yang, Xiaoou Tang, and Bolei Zhou. Interfacegan: Interpreting the disentangled face representation learned by gans. *IEEE transactions on pattern analysis and machine intelligence*, 2020.
- [54] Yujun Shen and Bolei Zhou. Closed-form factorization of latent semantics in gans. In *Proceedings of the IEEE/CVF Conference on Computer Vision and Pattern Recognition*, pages 1532–1540, 2021.
- [55] Vincent Sitzmann, Julien N.P. Martel, Alexander W. Bergman, David B. Lindell, and Gordon Wetzstein. Implicit neural representations with periodic activation functions. In *Advances in Neural Information Processing Systems (NeurIPS)*, 2020.
- [56] Vincent Sitzmann, Michael Zollhöfer, and Gordon Wetzstein. Scene representation networks: Continuous 3D-structure-aware neural scene representations. In *Advances in Neural Information Processing Systems (NeurIPS)*, 2019.
- [57] Jingxiang Sun, Xuan Wang, Yichun Shi, Lizhen Wang, Jue Wang, and Yebin Liu. Ide-3d: Interactive disentangled edit-

- ing for high-resolution 3d-aware portrait synthesis. *arXiv preprint arXiv:2205.15517*, 2022.
- [58] Jingxiang Sun, Xuan Wang, Yong Zhang, Xiaoyu Li, Qi Zhang, Yebin Liu, and Jue Wang. Fenerf: Face editing in neural radiance fields. In *Proceedings of the IEEE/CVF Conference on Computer Vision and Pattern Recognition*, pages 7672–7682, 2022.
- [59] Ayush Tewari, Mohamed Elgharib, Gaurav Bharaj, Florian Bernard, Hans-Peter Seidel, Patrick Pérez, Michael Zollhöfer, and Christian Theobalt. Stylerig: Rigging stylegan for 3d control over portrait images, 2020.
- [60] Omer Tov, Yuval Alaluf, Yotam Nitzan, Or Patashnik, and Daniel Cohen-Or. Designing an encoder for stylegan image manipulation. *ACM Transactions on Graphics (TOG)*, 40(4):1–14, 2021.
- [61] Zongze Wu, Dani Lischinski, and Eli Shechtman. Stylespace analysis: Disentangled controls for stylegan image generation. In *Proceedings of the IEEE/CVF Conference on Computer Vision and Pattern Recognition*, pages 12863–12872, 2021.
- [62] Weihao Xia, Yulun Zhang, Yujie Yang, Jing-Hao Xue, Bolei Zhou, and Ming-Hsuan Yang. Gan inversion: A survey. *arXiv preprint arXiv:2101.05278*, 2021.
- [63] Yinghao Xu, Sida Peng, Ceyuan Yang, Yujun Shen, and Bolei Zhou. 3d-aware image synthesis via learning structural and textural representations. In *Proceedings of the IEEE/CVF Conference on Computer Vision and Pattern Recognition (CVPR)*, pages 18430–18439, June 2022.
- [64] Yinghao Xu, Sida Peng, Ceyuan Yang, Yujun Shen, and Bolei Zhou. 3d-aware image synthesis via learning structural and textural representations. In *Proceedings of the IEEE/CVF Conference on Computer Vision and Pattern Recognition*, pages 18430–18439, 2022.
- [65] Linjie Yang, Ping Luo, Chen Change Loy, and Xiaoou Tang. A large-scale car dataset for fine-grained categorization and verification. In *Proceedings of the IEEE conference on computer vision and pattern recognition*, pages 3973–3981, 2015.
- [66] Oğuz Kaan Yüksel, Enis Simsar, Ezgi Gülperi Er, and Pinar Yanardag. Latentclr: A contrastive learning approach for unsupervised discovery of interpretable directions. In *Proceedings of the IEEE/CVF International Conference on Computer Vision*, pages 14263–14272, 2021.
- [67] Richard Zhang, Phillip Isola, Alexei A Efros, Eli Shechtman, and Oliver Wang. The unreasonable effectiveness of deep features as a perceptual metric. In *CVPR*, 2018.
- [68] Weiwei Zhang, Jian Sun, and Xiaoou Tang. Cat head detection - how to effectively exploit shape and texture features. In *European Conference on Computer Vision (ECCV)*, 2008.
- [69] Xuanmeng Zhang, Zhedong Zheng, Daiheng Gao, Bang Zhang, Pan Pan, and Yi Yang. Multi-view consistent generative adversarial networks for 3d-aware image synthesis. In *Proceedings of the IEEE/CVF Conference on Computer Vision and Pattern Recognition*, pages 18450–18459, 2022.
- [70] Jiapeng Zhu, Yujun Shen, Deli Zhao, and Bolei Zhou. In-domain gan inversion for real image editing. In *European conference on computer vision*, pages 592–608. Springer, 2020.
- [71] Jun-Yan Zhu, Philipp Krähenbühl, Eli Shechtman, and Alexei A Efros. Generative visual manipulation on the natural image manifold. In *European conference on computer vision*, pages 597–613. Springer, 2016.

A. Additional Results

A.1. Additional Real Image Editing Results

We show other real image editing results for MVCGAN. Thanks to the generator model’s high-resolution output, our editing results are also very high-resolution. In Fig. 10, we show results for face inversion and several attribute editings, *e.g.*, smiling, changing the hair color, and wearing eyeglasses. In all cases, our edits correctly maintain the 3D consistency of the generated face.

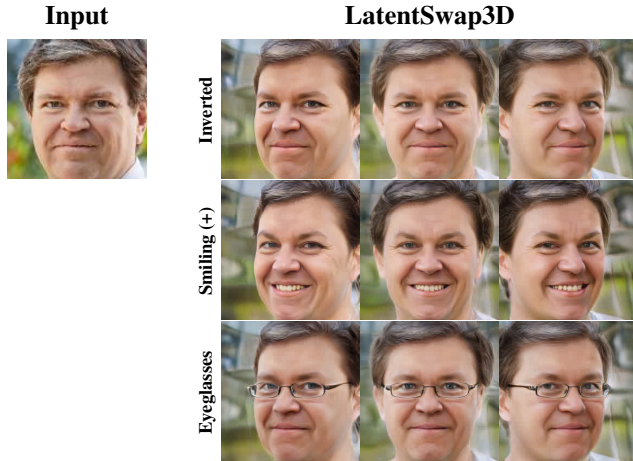


Figure 10. Additional inverted and edited examples from our approach on MVCGAN.

A.2. Additional AFHQ Editing

In Fig. 11, we show additional qualitative results on applying edits to samples generated from models trained on AFHQ [10] - Dogs dataset. We use the attribute classifiers presented in Appendix D.3 to identify the dimension to edit. Note that even if the classifiers are trained on cat images, they can successfully be used for attribute editing on dog images.

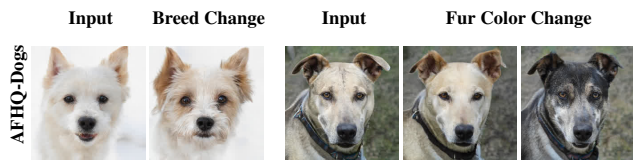


Figure 11. Results for AFHQ dataset [10], for dog images, from LatentSwap3D on StyleGAN2.

A.3. LatentSwap3D on Other 3D-aware Generators

VolumeGAN is a high-quality 3D-aware generative model explicitly trained to learn a structural and a textural representation, and it is based on NeRF [63]. The results of our approach on VolumeGAN - FFHQ are provided

in Fig. 12. Our approach applies the desired attributes, *e.g.*, removing eyeglasses, changing the hair color, and reducing the facial hair, to the latent space of VolumeGAN, without changing the identity of the input face.

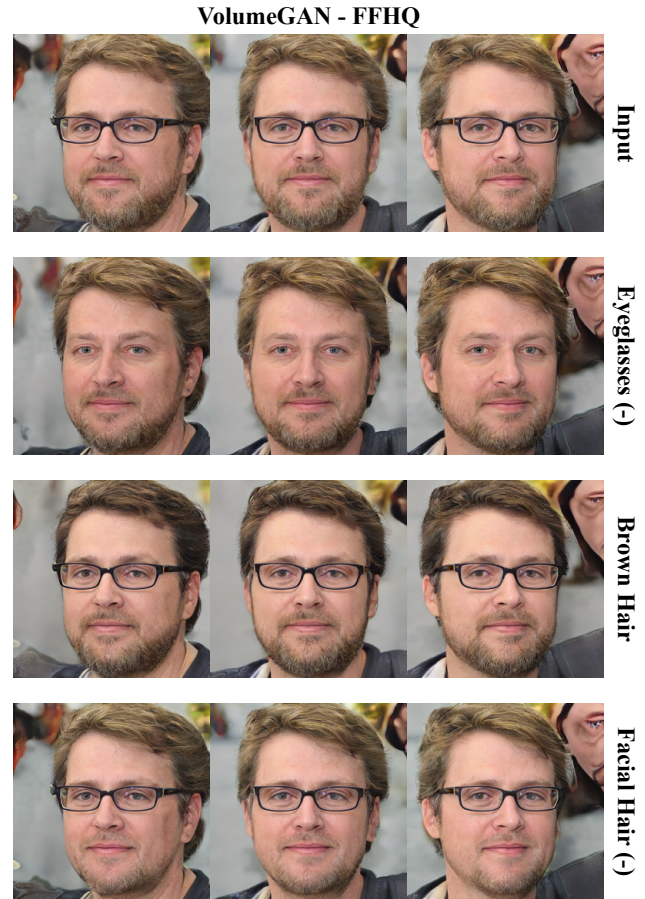


Figure 12. LatentSwap3D on VolumeGAN [64] - FFHQ.

GIRAFFE consists of NeRF and 2D GANs. The NeRF part outputs the features of the 3D shape and texture, while the 2D GAN part outputs the final image [37].

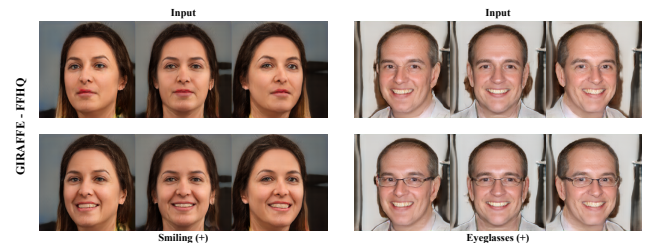


Figure 13. LatentSwap3D on GIRAFFE [37] - FFHQ

Figure 13 show smiling and wearing eyeglasses edits from LatentSwap3D on the GIRAFFE - FFHQ model



Figure 14. LatentSwap3D on GIRAFFE [37] - CompCars [65].

following the same protocol detailed for the other FFHQ trained generators. To test how well LatentSwap3D generalizes to different datasets, we extended the experiment to include CompCars [65] using the pre-trained GIRAFFE generator. Furthermore, due to the lack of classifiers for car attributes, as a proof of concept, we trained a ResNet-50 to classify the color of a car from scratch on Myauto.ge Cars Dataset [36]. As seen from Fig. 14, using these classifiers, our approach can edit the color of the cars successfully.

StyleNeRF is another high-resolution 3D-aware generative model that integrates a NeRF into a 2D style-based generator [18]. StyleNeRF is able to generate high-resolution and 3D consistent images/shapes from unstructured 2D images. Figure 15 shows our attribute editing, *e.g.*, smiling, removing bangs, and changing the hair color on StyleNeRF - FFHQ.

A.4. Additional Comparison to Other Methods

In addition to Fig. 7, we report here an additional comparison among LatentSwap3D, InterFaceGAN [53] and StyleFlow [2]. As seen in Fig. 16, our approach provides meaningful semantic edits without changing the identity on the input image and performs best for all the desired attributes among 3D-aware generative models. In contrast, the other methods may change the identity or make entangled edits.

A.5. Additional Quantitative Analysis

We report *Distribution-level Image Quality* metrics in addition to *Identity Preservation*, Tab. 3, and *Semantic Correctness*, Tab. 2, metrics. We calculate Frchet Inception Distance (FID) [22, 51] and Kernel Inception Distance (KID) [4] between 10K edited images and the CelebA test dataset for the face domain and AFHQ test dataset for the animal domain. Although our method does not have the best FID and KID metrics, it is on par with other methods.

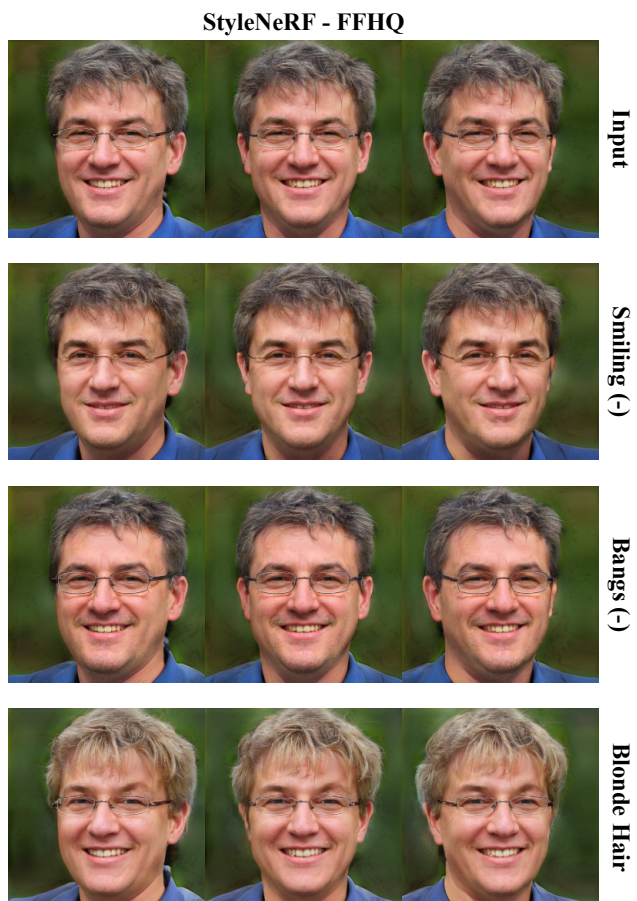


Figure 15. LatentSwap3D on StyleNeRF [18] - FFHQ.

Since these metrics do not indicate the methods' editing capability, our method's results are acceptable. The results of InterFaceGAN are better than those of unedited images. One explanation for these findings can be that InterFaceGAN changes the identity of the generated images and creates a more diverse image set.

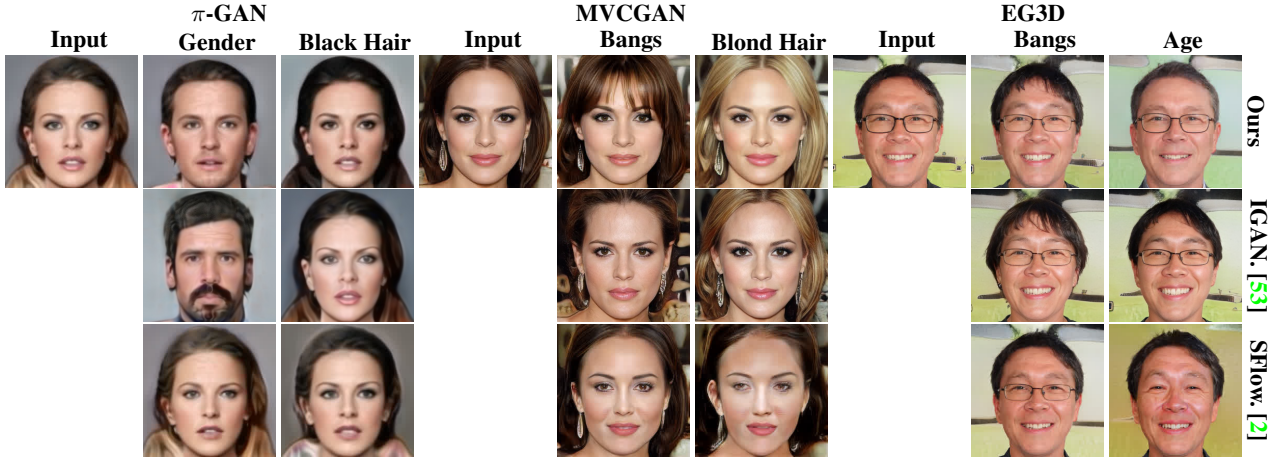


Figure 16. Detailed comparison to other methods for π -GAN, MVCGAN and EG3D. The edited attributes are annotated.

Method	π -GAN				MVCGAN				EG3D			
	CelebA		Cats		FFHQ		AFHQ		FFHQ		AFHQ	
	FID	KID										
Unedited	50.7	0.045	57.4	0.055	54.1	0.048	47.1	0.041	47.5	0.039	39.5	0.037
LCLR.	53.4	0.051	60.1	0.062	55.6	0.052	51.2	0.047	59.6	0.049	40.1	0.031
SeFa	68.2	0.062	59.2	0.059	69.4	0.063	49.2	0.045	64.3	0.051	44.1	0.038
IGAN.	48.9	0.034	59.6	0.059	62.3	0.056	53.1	0.039	58.8	0.053	45.8	0.039
SFlow.	52.1	0.047	59.1	0.058	56.3	0.051	50.8	0.041	60.2	0.049	40.4	0.034
Ours	51.2	0.048	58.8	0.057	60.8	0.053	50.3	0.041	61.1	0.051	42.1	0.035

Table 4. Quantitative comparison of FID and KID among different image editing methods for π -GAN, MVCGAN, and EG3D on attribute edits of face and animal images. The selected attributes are mentioned in Appendix D.4.

B. Ablation Studies

This section reports some ablation studies on tuning the number of dimensions K that will be swapped, a study on alternative latent space edit methods: linear operations and direct optimization of the desired attribute, and a comparison on the use of random forests vs. other ranking methods for latent dimensions ranking. For these experiments we use π -GAN [8] and StyleSDF [38].

B.1. Impact of parameter K

Figure 17 shows a qualitative example that emphasizes the impact of the number of dimension K swapped for two attribute edits. Higher K values increase the edit’s strength but simultaneously result in images less similar to the original. The percentage reported above/below each sample shows the value of identity loss \mathcal{L}_{ID} , in Fig. 17. Increasing K results in images less similar to the input image but more similar to the supported image. We automatically set K for

each sample being edited such that \mathcal{L}_{ID} does not go above 30% for face datasets and 10% for other domains (animals). The rightmost faces are the most similar in the support set.

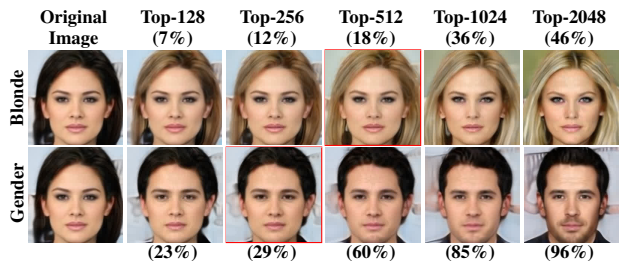


Figure 17. The % corresponds to the identity loss \mathcal{L}_{ID} between edited and original as described in Sec. 3.4

B.2. Alternative Edit Techniques

Linear operations: Style-based generators use AdaIN [23] layers to guide the image generation pro-

cess. AdaIN layers apply a linear transformation to the input features; therefore, they are suitable to be modified with simple linear transformations in the latent space. For example, recently [61] showed that such linear operations are enough to provide disentangled and fine-grained manipulations in the latent space of StyleGAN2 [28]. π -GAN and StyleSDF use SIREN [55] layers that, due to the presence of sin-based activation functions, enforce periodicity in the learned latent space. Intuitively linear edits of latent codes (such as additions or subtractions) will not perform nicely in a periodic latent space, therefore motivating the need to resort to the feature swapping mechanism of LatentSwap3D. To experimentally verify this intuition, we have conducted an ad-hoc experiment performing linear operations, such as addition and subtraction, on the latent spaces of π -GAN and StyleSDF and reported the results in Fig. 18. Linear edits in this context are defined as constant changes on the top 256 features ranked from our trained Random Forests. To increase or decrease the corresponding latent codes, we look at the sign of the difference between the latent codes of the image that will be edited and the support images that have the desired attribute. Linear operations on π -GAN can result in images with some artefacts (e.g., π -GAN - smiling) or lower intensity edits (e.g., π -GAN - black hair). For StyleSDF, linear operations can apply the desired edit and generate realistic images but have an undesired side effect on the edited image’s identity. The StyleSDF - female edit changes the background and clothing, while the StyleSDF - age edit also changes the hairstyle.

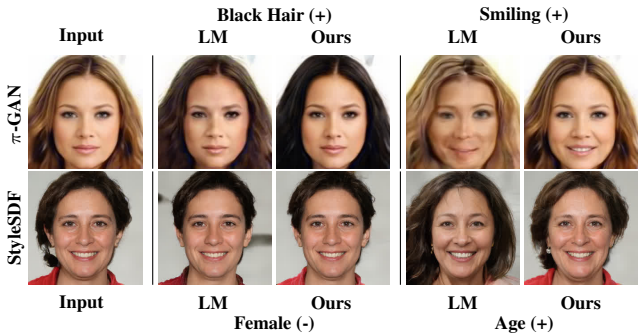


Figure 18. Effect of linear manipulations (LM) on the latent space of the 3D-aware generative models, π -GAN and StyleSDF.

Direct optimization: Since we have differentiable image classifiers for the attribute we would like to edit, an alternative to LatentSwap3D would be to directly optimize latent codes to maximize the presence of the desired attribute as measured by the respective classifiers. To com-

pare against this alternative, we first trained binary image classifiers based on ResNet-50 [21] on the CelebA [32] dataset for each attribute. Then, we take the latent codes of the original image as the initial point and try to learn an offset in the latent space that, when summed to the initial latent code, applies the desired transformation. To optimize the offset, we feed the generator the original latent code modified by the offset, generate an edited image, and provide it to the attribute classifier. At this point, we can compute as a loss function the cross-entropy loss between the output of the classifier and the class of the desired attribute and minimize it to optimize the offset using back-propagation directly. For the optimization procedure, we perform 400 iterations with Adam [29]. As shown in Fig. 19, this method struggles to preserve the identity of the edited image (see all lines). Moreover, it learns edits that are not realistic but are classifier-biased, such as the smiling (+) attribute that brightens the teeth. In contrast, the smiling (-) attribute changes the color of the teeth to the skin color; see light-green arrows in Fig. 19.

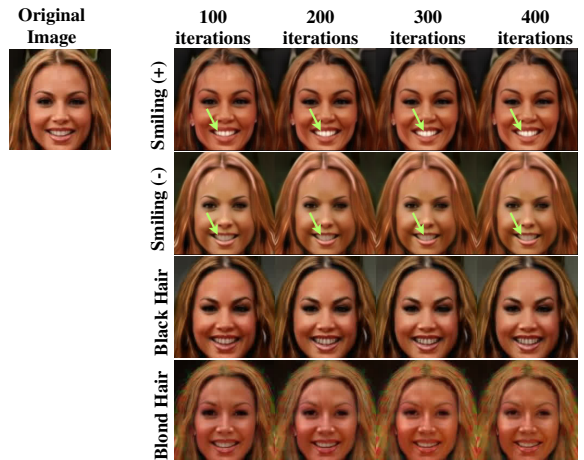


Figure 19. Attribute edits obtained by directly optimizing the latent codes using pre-trained image classifiers and back-propagation.

B.3. Other Feature Ranking Methods

In LatentSwap3D, we use Random Forests [5] based feature ranking; in this section, we experimentally motivate this choice by considering other methods for feature ranking. We consider three alternatives: (i) the *SelectKBest* [41] method from the popular SciKit-Learn library that sorts the feature based on a score function, such as χ^2 [40], and selects the k features with the highest scores, (ii) *Support Vector Machine* (SVM) [11] based method that takes the absolute values of the feature coefficients of a trained linear SVM, and (iii) *SHapley Additive exPlanations* (SHAP) [33] based method that explains the output of trained machine learning models by calculating the importance of the fea-

tures. As can be seen in Fig. 20, SHAP- and RF-based methods show similar performance on the attributes *female* (-), *smiling* (+). However, for *blondness* (+) and *makeup* (+) attribute edits, the random forest-based ranking provide higher quality. On the other hand, SVM-based ranking has comparable results for *smiling* (+) and *makeup* (+), but for the other attributes fails to generate the corresponding edits. Finally, the *SelectKBest* method performs similarly to the SVM-based ranking method, but it has a small effect on the blondness attribute. For all methods, the parameter K for swapping is optimized separately using the identity loss discussed in Appendix B.1.

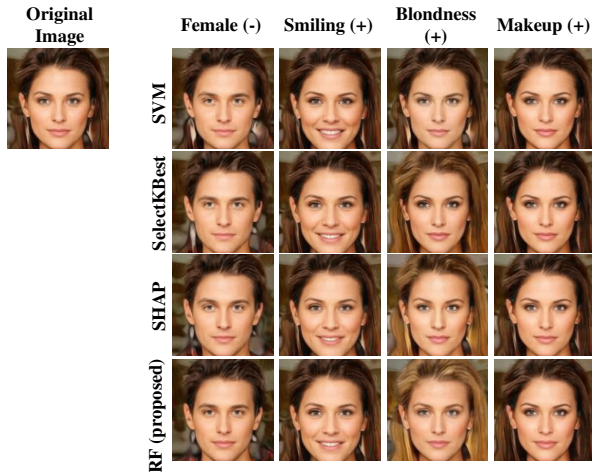


Figure 20. Comparison of various feature ranking methods on the latent space of π -GAN.

B.4. Details on Camera Pose Optimization

Using off-the-shelf face pose estimation can be an alternative to the proposed method for the specific case of faces. However, it will hinder the generalizability of the inversion procedure to only those datasets or object categories for which a pose estimator can be trained. Our alternating optimization schema, instead, only relies on the assumption of having a trained generator and, as such, provides a more general solution. To show the impact of optimizing the pose on the inversion process, we report a comparison in Fig. 21.

C. Limitations

Under-represented Attributes on Training Datasets of GANs. During the development of this work, we identified some attribute manipulations that cannot be applied in the latent space of pre-trained 3D-aware image generators. These usually cover under-represented classes in the original training set, such as faces with a hat or earrings. We hypothesize that these samples fall out of distribution for the generator, and as such, they do not have specific dimensions in the latent space allocated to them. For this reason,

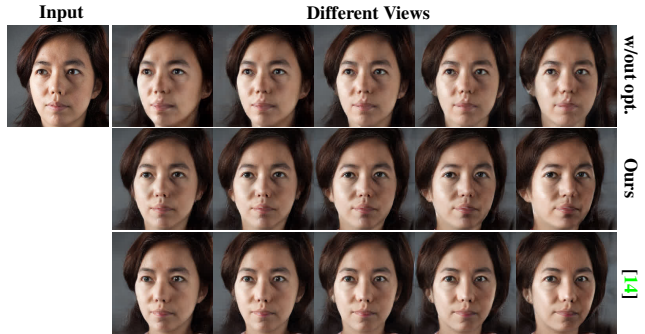


Figure 21. Importance of Camera Optimization in Inversion Procedure. Off-the-shelf pose estimator [14].

reproducing them with our editing technique is difficult. We show some failed edits in Fig. 22.

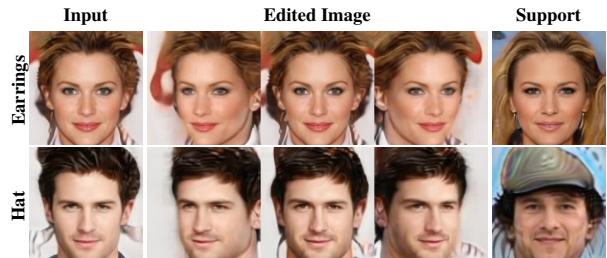


Figure 22. Failure edits on the latent space of π -GAN for classes under-represented in the training set.

Real Images Inverting Capabilities of GANs. We showed promising initial results on editing real images via GAN inversion followed by LatentSwap3D. During the development of this work, we found that the inversion of an image in the latent space of 3D generators is quite challenging and sometimes fails to generate high-quality outputs or maintain the identity of the inverted face. This is particularly true for StyleSDF, where the inverted faces resemble the original but not perfectly. For example, we show one inversion in Fig. 23. However, with the better inversion capabilities, e.g., MVCGAN, our model is able to produce better attribute editing on the real images.



Figure 23. Result from inversion on the latent space of StyleSDF. As can be observed the inverted image matches the global appearance of the original one but not the identity.

Supervised Method for Finding Semantic Edits. LatentSwap3D relies on the ability to train attribute classifiers to identify and rank the relevant dimensions in the latent space that controls the desired attribute. Our method can only be applied if we successfully train such attribute classifiers. For most of our experiments, we relied on pre-trained attribute classifiers to pseudo-label generated images with the presence or absence of the desired attribute bypassing this problem. Nevertheless, for new attributes for which a pre-trained classifier is unavailable, the generated images would need to be manually labeled, increasing the time required to apply our method. Fortunately, the random forest classifiers we use to rank features do not require massive training sets and can be easily trained with a few hundred labeled samples.

D. Implementation Details

D.1. Datasets

We test our proposed model, LatentSwap3D, with 3D-aware generative models on images from six different datasets: CelebA (256x256) [32], FFHQ (1024x1024) [27], Cats (256x256) [68], AFHQ (512x512) [10], and CompCars [65] (256x256) method to the 2D GAN model StyleGAN2 on FFHQ (1024x1024) [27], AFHQ (512x512) [10], and MetFaces (1024x1024) [25].

CelebA is a large-scale dataset that contains more than 200K face images of over 10K different celebrities and 40 annotated attributes for each image [32]. It has a resolution of 256x256. π -GAN and MVCGAN provide pre-trained weights for CelebA.

FFHQ dataset consists of over 70K high-resolution (1024x1024) and high-fidelity images of human faces [27]. The dataset has diverse samples regarding age, ethnicity, and wearing accessories. It is used in this work to generate images from StyleNeRF, VolumeGAN, GIRAFFE, StyleSDF, MVCGAN, and EG3D.

Cats contains 6K images of cat heads [68]. Its resolution is 128x128. The dataset is used to generate cat images from π -GAN.

AFHQ is a dataset that contains over 15K high-resolution (512x512) and high-quality images of animal faces [10]. The dataset has three domains: dogs, cats, and wildlife animals, and each domain has 5K samples. MVCGAN, EG3D, and StyleSDF have pre-trained weights for AFHQ.

MetFaces consists of over 1K human faces (1024x1024) extracted from works of art. The images are automatically aligned and cropped [25]. This dataset is used only when evaluating LatentSwap3D on StyleGAN2.

CompCars contains 1716 car models and a total of 137K images of cars [65]. Its resolution is 256x256. This dataset is used only when evaluating LatentSwap3D on GIRAFFE.

D.2. Runtime Analysis

LatentSwap3D consists of two main steps, as shown in Fig. 2a and Fig. 2a. We measure the runtime on an NVIDIA Tesla T4 GPU Machine with 12 cores.

Method	Discovering Step	Editing Step	Image Inversion
π -GAN	180 min.	600 ms/im.	20 min./im.
MVCGAN	68 min.	600 ms/im.	8 min./im.
EG3D	72 min.	600 ms/im.	8 min./im.

Table 5. Overall runtime analysis of the proposed method. The values for the first column are calculated using a dataset of 10K generated images.

Discovery of Relevant Latent Dimensions. For the step in Sec. 3.3, there are three main processes: **(i)** generating the training set from random sampling in the latent space of the generator, **(ii)** predicting the probabilities of the presence of the desired attribute in the generated images using pre-trained image classifiers, and **(iii)** training a random forest to predict the presence of the selected attribute from the latent codes. Considering π -GAN as a generator, the image generation step takes 2 hours for 10K images, while for MVCGAN and EG3D, it takes 8 minutes and 12 minutes, respectively. Labeling the 10K images using the pre-trained image classifiers takes 45 seconds per attribute. Finally, the training process of the random forests takes 1 minute per attribute.

Attribute Editing on Latent Dimensions. The second step is described in Sec. 3.4. On average, we need around 600 milliseconds per image for all generators.

3D Edits on Real Images. The runtime analysis for the inversion of real images for each generator is shown in Tab. 5. The inversion procedure can be sped up using encoder-based inversion approaches. However, we leave it to future development.

D.3. Details of Animal Attribute Classifiers

We trained ResNet-50 [21] classifiers to predict *Siamese breed* and *brown color* by using the dataset [44]. Since we do not have frontal and zoom-in views of the animals, we apply a haar detector¹ for cat faces for the dataset. Our model can successfully edit AFHQ and Cats datasets by leveraging these attribute classifiers.

¹https://github.com/kipr/opencv/blob/master/data/haarcascades/haarcascade_frontalface_default.xml

D.4. Details on the Quantitative Analysis

For *Distribution-level Image Quality* and *Identity preservation* metrics, we use 2000 generated images per attribute from five different attributes. For LatentSwap3D, InterFaceGAN [53], and StyleFlow [2], we select the attributes for the three generators as follows: for π -GAN we tested *gender, smile, age, hair color, and heavy makeup*, while for MVCGAN and EG3D, we picked *gender, smile, age, glasses, and adding beard*. SeFa [54] and LatentCLR [66] are unsupervised edits discovery methods. Therefore, we cannot isolate specific attribute editing transformations. So instead, we take the top five *semantics* for SeFa and five *directional models* for LatentCLR.

D.5. Details on the Comparison to Other Methods

Since the other 3D editing methods apply to specific architectures or have their generator part, we pick 2D attribute manipulators that have been proven to work well on 2D generators as baselines. They can also be applied to latent spaces of 3D GANs. InterFaceGAN [53] and StyleFlow [2] are the closest competitors to our method and were originally proposed for image generators. Similarly to LatentSwap3D, InterFaceGAN leverages pre-trained attribute classifiers to find the corresponding linear edit directions in the latent space of trained generators. However, as mentioned, linear edits are sub-optimal in the periodic space determined by the SIREN [55] activation functions used in π -GAN and MVCGAN. On the other hand, StyleFlow uses the attribute information during the training of normalizing flows as conditions. For example, when editing the desired attribute on a face sample, the user can give the desired attribute as a condition. In our comparison, we also consider methods for unsupervised discovery of editing directions: SeFa [54] and LatentCLR [66]. Both methods do not have assumptions about the characteristic of the generator to which they are applied. Therefore, they can be easily adapted to NeRF-based generators like π -GAN or MVCGAN.

E. Future Work

Real Images Inverting Capabilities of GANs. While a better 3D-aware GAN inversion was outside the scope of this work, we believe that in the future, some of the proposed techniques for style-based 2D generators like [48] could be adapted for the new category of 3D-aware generators and combined with LatentSwap3D to enable even more powerful edits on real images. For instance, if encoder-based inversion [48] is adapted, it will speed up the inversion process.

Improvement on Disentanglement. As an exciting direction to overcome the limitation of the improvement of

disentanglement, we plan to explore a way of constraining the latent space of NeRF-based GAN models to exhibit such disentanglement properties. Similar paths have been recently proposed for style-based generators [19].

Finding Semantic Edits by Unsupervised or Self-supervised Manner. This study is one of the pioneers for conducting semantic edits in 3D-aware generative models. Therefore, future studies can work on adapting the 2D unsupervised and self-supervised image manipulators like [39, 54, 66], to provide unsupervised methods for finding semantic edits.